Materials Science and Engineering, A181/A182 (1994) 1227–1231

Comparison of the transformation sequence from γ-AlOOH (boehmite) to α-Al_2O_3 (corundum) induced by heating and by ball milling

A. Tonejc, A. M. Tonejc and D. Bagović

Department of Physics, Faculty of Science, PO Box 162, 41001 Zagreb (Croatia)

C. Kosanović

Ruder Bošković Institute, PO Box 1016, 41001 Zagreb (Croatia)

Abstract

This paper presents the X-ray diffraction investigation of ball-milling-induced transformation of boehmite (γ-AlOOH) and of gibbsite ($Al(OH)_3$) to corundum (α-Al_2O_3). The results are compared with the transformation observed in heating experiments, and the conclusion is drawn that equivalence exists between the high energy ball milling and the thermal process.

1. Introduction

In a recent publication [1] we have shown that the well-known temperature-induced transition from γ-boehmite (γ-AlOOH) to corundum (α-Al_2O_3) [2–6] could also be obtained by high energy ball milling. Since, upon heating, the transformation of boehmite to corundum occurs over a series of transition phases, in the present experiment an attempt is made to compare the heating- and milling-induced transition sequences.

Heating of boehmite or of gibbsite ($Al(OH)_3$) at over 1000 °C yields a variety of transition aluminas before the stable corundum is formed [2–6]:

$$\underset{\text{(gibbsite)}}{Al(OH)_3} \xrightarrow{>170\,^{\circ}C} \chi\text{-}Al_2O_3 \xrightarrow{>500\,^{\circ}C} \kappa\text{-}Al_2O_3 \xrightarrow{>825\,^{\circ}C} \alpha\text{-}Al_2O_3 \qquad (1)$$

$$\underset{\text{(boehmite)}}{\gamma\text{-}Al(OOH)} \xrightarrow{>350\,^{\circ}C} \gamma\text{-}Al_2O_3 \xrightarrow{>600\,^{\circ}C} \delta\text{-}Al_2O_3 \xrightarrow{\approx 900\,^{\circ}C} \theta\text{-}Al_2O_3 \xrightarrow{>1000\,^{\circ}C} \alpha\text{-}Al_2O_3 \qquad (2)$$

The transition temperatures are somewhat approximate, but it is worth remembering that, although all transition aluminas are stable at room temperature, they are normally activated only at above-indicated temperatures and cannot be retraced in reverse with decreasing temperature.

2. Experimental procedure

A commercial boehmite powder (Ventron, Karlsruhe) and a synthetic gibbsite (Aluminium Factory, Mostar) were used as starting materials. The heating was performed in a well-temperature-controlled furnace, and the milling in a Fritsch planetary ball mill. Both the vial and the balls were made of tungsten carbide (WC). A 1 g mass of powder and a set of ten balls with a diameter of 10 mm were used in all experiments. For every milling experiment a new charge of starting powder was used and then milled uninterruptedly for the imposed time intervals. Before and after the heating or milling, the powders were examined using a Philips PW 1820 X-ray diffractometer with Cu Kα monochromated radiation. Transmission electron microscopy (TEM) observations were performed on a JEOL JEM 2010 microscope.

3. Results

3.1. Heating

The diffuse characteristic and the similarity of X-ray diffraction (XRD) patterns of non-milled alumina powders were the main reason that we also performed the heating experiments in order to be able to determine which of the transition aluminas appeared in the milling-induced boehmite- or gibbsite-to-corundum transition. We performed several heating experiments 200 h long which confirmed the facts [5, 6] that the transition phases of the aluminas are stable below the transition temperature and that diffuse broad lines persist even after long heating.

In Fig. 1, those XRD patterns which we found to be the most important in identifying the phases in milled powders are shown. The boehmite and the gibbsite

0921-5093/94/\$7.00
SSDI 0921-5093(93)05661-8

transformation sequences obtained by heating and deduced from our XRD patterns were

$$\text{boehmite} \xrightarrow{>300\,^\circ\text{C}} \gamma\text{-Al}_2\text{O}_3 \xrightarrow{>700\,^\circ\text{C}} \delta\text{-Al}_2\text{O}_3 \xrightarrow{>800\,^\circ\text{C}} \theta\text{-Al}_2\text{O}_3 \xrightarrow{>850\,^\circ\text{C}} \alpha\text{-Al}_2\text{O}_3$$

$$\text{gibbsite} \xrightarrow{>250\,^\circ\text{C}} \chi\text{-Al}_2\text{O}_3 \xrightarrow{>650\,^\circ\text{C}} \kappa\text{-Al}_2\text{O}_3 \xrightarrow{>800\,^\circ\text{C}} \alpha\text{-Al}_2\text{O}_3$$

and are in agreement with the published data (sequences (1) and (2)).

3.2. Milling

Figures 2 and 3 show a series of XRD patterns of the boehmite and of the gibbsite powders subjected to milling for different milling times. Although the

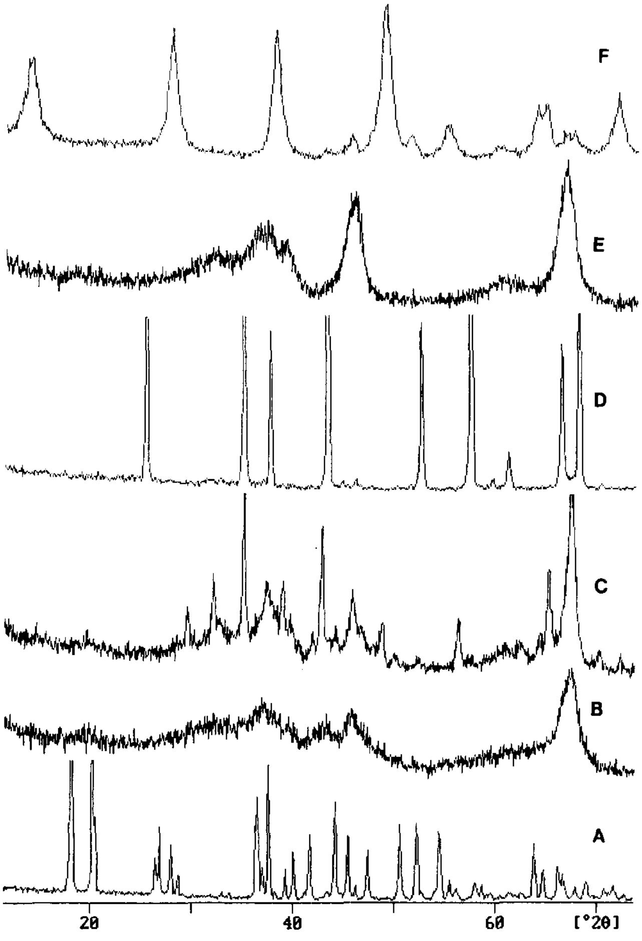

Fig. 1. XRD patterns: curve A, gibbsite, as supplied; curve B, gibbsite heated at 500 °C for 200 h, χ-Al$_2$O$_3$; curve C, gibbsite heated at 800 °C for 200 h, κ-Al$_2$O$_3$; curve D, gibbsite and boehmite heated at 1300 °C for 3 h, α-Al$_2$O$_3$; curve E, boehmite heated at 500 °C for 200 h, γ-Al$_2$O$_3$; curve F, boehmite, as supplied. The diffraction intensity is measured in counts (arbitrary units).

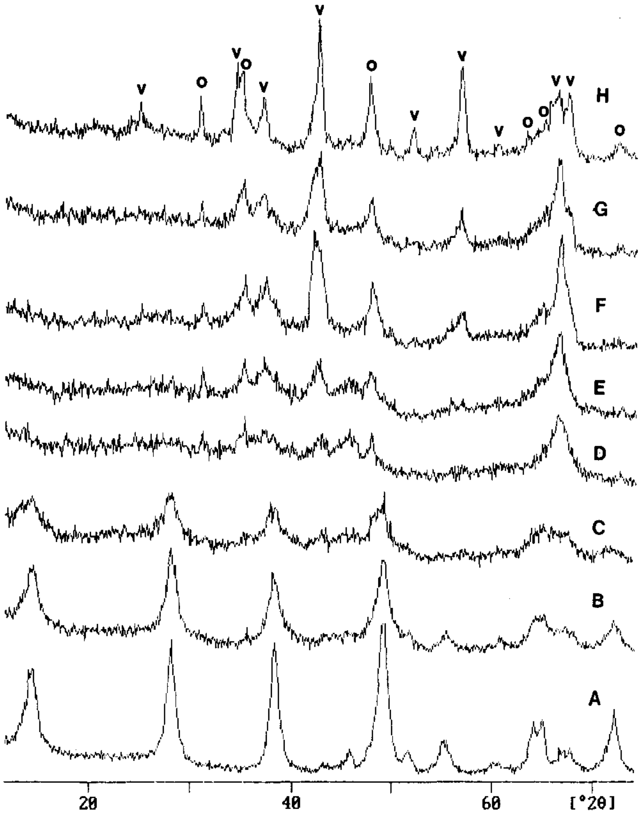

Fig. 2. Changes in XRD pattern for boehmite powders with various milling times (v, α-Al$_2$O$_3$; o, WC): curve A, 0 min; curve B, 10 min; curve C, 20 min; curve D, 40 min; curve E, 60 min; curve F, 90 min; curve G, 120 min; curve H, 250 min. The diffraction intensity is measured in counts (arbitrary units).

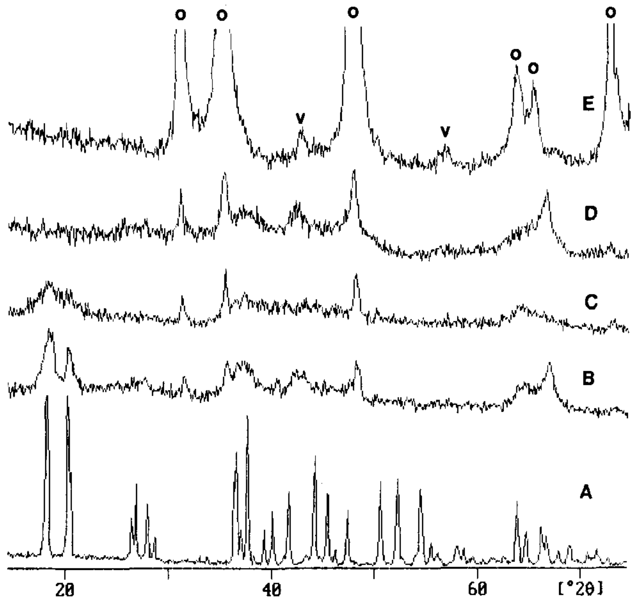

Fig. 3. Change in XRD pattern of gibbsite powders with various milling times: (v, α-Al$_2$O$_3$; o, WC): curve A, 0 h; curve B, 0.5 h; curve C, 1.5 h; curve D, 2.5 h; curve E, 7 h. The diffraction intensity is measured in counts (arbitrary units).

patterns showed very broad maxima, with the aid of XRD patterns obtained in heating experiments (Fig. 1) we were able to identify the phases which appeared during milling.

It is clear that the intensities of the boehmite and gibbsite diffraction peaks weakened and broadened at the very beginning of the milling. However, before the boehmite (or the gibbsite) maxima completely disappeared, a broad maximum belonging to the χ-Al_2O_3 phase could be observed. On further milling of the boehmite, broad peaks of the χ phase gradually disappeared and the peaks of the κ phase appeared. On further milling, α-Al_2O_3 peaks appeared and gained intensity while those belonging to the κ phase gradually disappeared. On milling the boehmite for 1.5 h the corundum diffraction lines could be observed on XRD patterns, but for gibbsite the corundum lines were observed after milling for 7 h.

The peaks of WC became visible on XRD patterns of both boehmite and of the gibbsite powder milled for 30 min, indicating contamination of milled powders caused by the wear of balls and of the vial. For longer milling, the WC contamination was of such a high level that it could even mask the milling results of the original powders. The contamination turned out to be very drastic during the milling of the gibbsite. We suppose that this contamination prevented us from observing the κ phase during the milling of the gibbsite.

3.3. Transmission electron microscopy and high resolution electron microscopy

The boehmite used in the ball-milling as the starting powder and examined by high resolution electron microscopy (HREM) has very fine grains from 1.5 to 2.5 nm (Fig. 4). The corresponding selected-area diffraction (SAD) pattern is given in Fig. 4 as the inset, showing partly amorphous material A and partly crystalline material. The boehmite rings belonging to reflections (031), (131) and (002) are indicated in the SAD pattern, and the rows of white dots having a spacing of 0.198 nm and belonging to (131)-type boehmite planes are imaged (see inset). The boehmite appears to be beam sensitive and, during electron microscopy observation, γ-Al_2O_3 spots develop on boehmite rings in the SAD pattern. In the inset of Fig. 4, the rows of white dots have a 0.453 nm spacing which correspond to the spacing of the (111)-type planes in γ-Al_2O_3. The fine-grained boehmite observed in Fig. 4 provides an explanation for broad boehmite lines on XRD pattern (Fig. 2, curve A).

Low magnification view of α-Al_2O_3 powders, produced by the milling of boehmite for 2.5 h, together with the corresponding SAD pattern and qualitative energy-dispersive X-ray analysis (energy-dispersive spectroscopy (EDS)), is shown in Fig. 5. The SAD pattern of α-Al_2O_3 shows (012), (104), (110) and (113) reflections, revealing a polycrystalline distribution of α-Al_2O_3 grains. Separate grains having sizes from 15 to 200 nm could be seen. Since XRD patterns of the milled sample showed an appreciable amount of WC contamination, the regions observed by TEM were controlled by EDS to be sure that we are examining Al_2O_3 powders. Small traces of copper appeared because of the copper grids. Every particle seen on a micrometre scale analysed by TEM, as in Fig. 5, was composed of small crystallites having a nanometre range (Fig. 6).

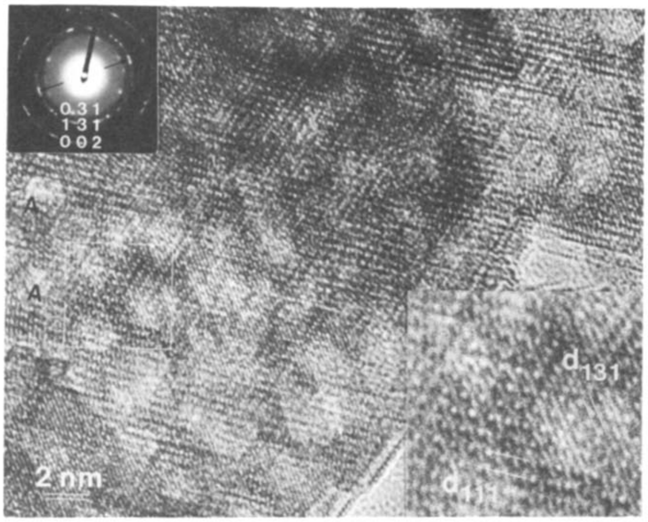

Fig. 4. High resolution electron micrograph of very-fine-grained (1.5–2.5 nm) boehmite powders used in ball milling with corresponding SAD pattern, showing partly amorphous material A and partly crystalline material. The lattice image of (131) boehmite (d=0.198 nm), and (111) of γ-Al_2O_3 (d=0.45 nm), are given in the insert.

The distribution of nanocrystals of α-Al_2O_3 having sizes from 4 to 16 nm with the lattice planes differently oriented is shown in Fig. 6. So, in grain A in Fig. 6, lattice planes (042) with an interplanar spacing d=0.344 nm and lattice planes (104) in grain C with d=0.255 nm are imaged with two-dimensional resolution; at intersections of these two families of planes, the atoms lying in these planes are separated by 0.255 nm and 0.344 nm respectively. The (116) planes with 0.160 nm spacings, are resolved in region B (Fig. 6).

In Fig. 7, the transmission electron micrograph and SAD pattern of α-Al_2O_3 obtained by heating the boehmite powder for 3 h at 1300 °C are shown (the corresponding XRD pattern is given in Fig. 1, curve D).

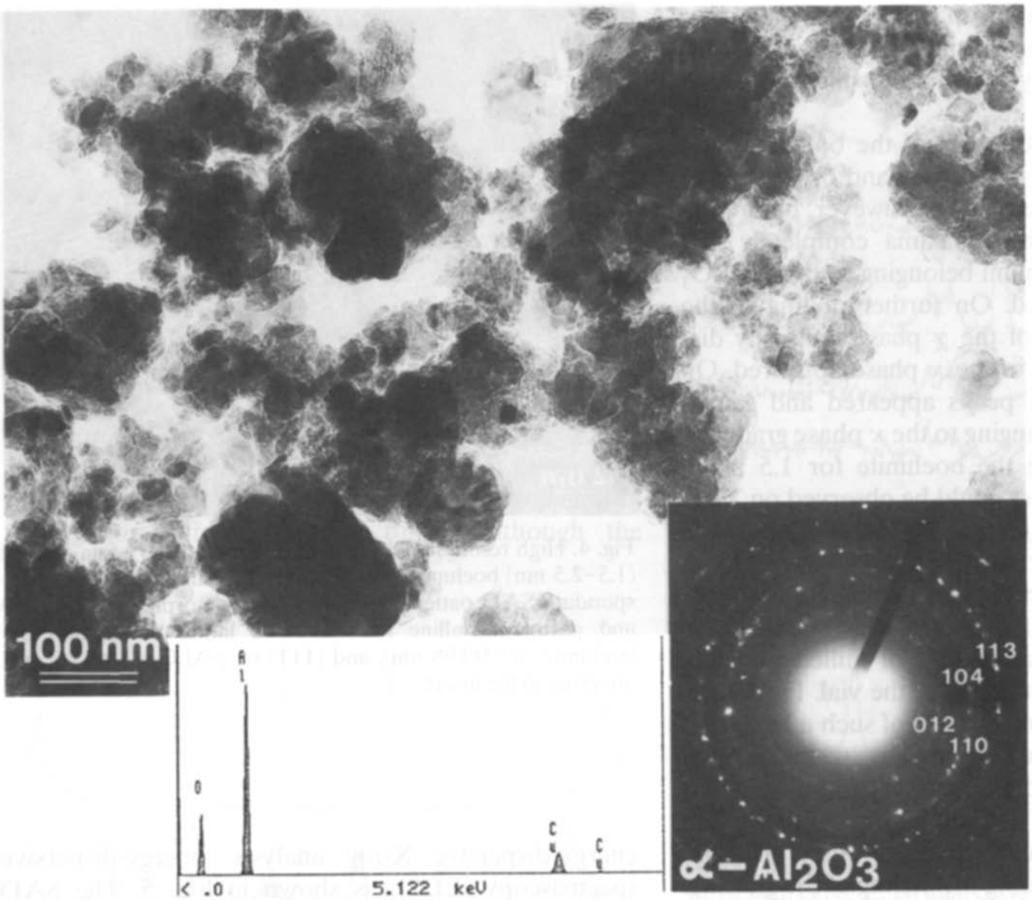

Fig. 5. Low magnification view of α-Al_2O_3 powders produced by milling the boehmite for 2.5 h, together with the EDS and SAD pattern of the examined area. Grain sizes from 15 to 200 nm can be seen.

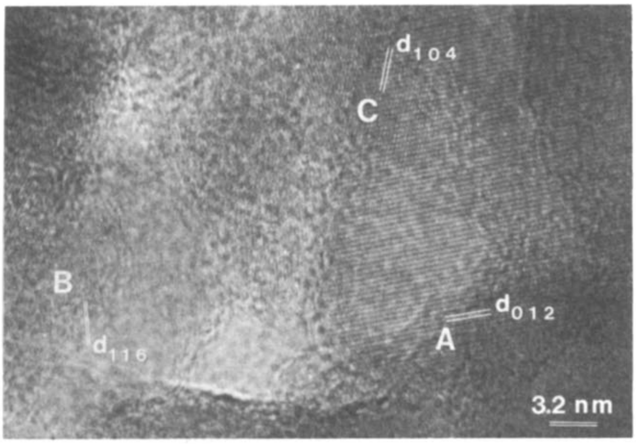

Fig. 6. High resolution electron micrograph of α-Al_2O_3. The lattice planes (012), (104) and (116), having interplanar spacings d of 0.344 nm, 0.255 nm and 0.160 nm respectively are imaged in the α-Al_2O_3 obtained by ball milling of the boehmite.

The large thick single crystal A which has some transparent edges and a size greater than 100 nm is oriented in the $[\bar{1}10]$ direction. The grains shown in Fig. 7 were not suitable for HREM examination.

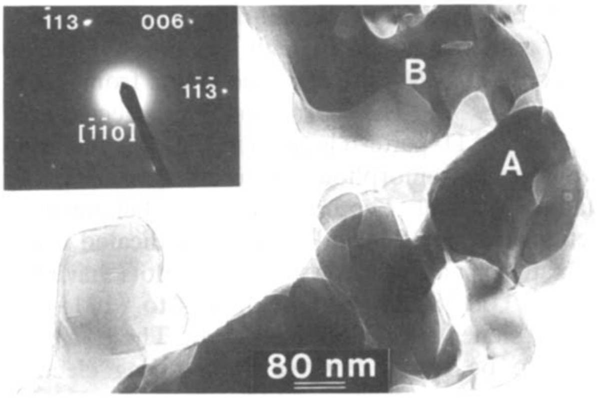

Fig. 7. Transmission electron micrograph and SAD pattern of α-Al_2O_3 obtained by heating the boehmite powder for 3 h at 1300 °C.

4. Discussion

Although very high temperatures (over 900 °C) are needed to transform gibbsite (or the boehmite) to stable corundum, we undoubtedly showed that this transformation could be obtained by ball milling also.

Irrespective of whether the starting powder was gibbsite or boehmite, the ball-milling-induced transformation sequence found was

$$\left.\begin{array}{l}\text{boehmite}\\ \text{gibbsite}\end{array}\right\} \rightarrow \chi\text{-Al}_2\text{O}_3 \rightarrow \kappa\text{-Al}_2\text{O}_3 \rightarrow \alpha\text{-Al}_2\text{O}_3 \qquad (3)$$

showing the similarity of ball-milling- and heating-induced transitions of boehmite and of the gibbsite.

In their work, Trudeau *et al.* [7] showed that the transformations induced by a thermal process can be very different. However, our experiments showed on the contrary that the thermal-process-induced and high energy ball-milling-induced transformations could be equivalent. Although temperatures higher than 1100 °C are required to produce α-Al_2O_3 within a few hours, and regardless of the controversy regarding the so-called "local effective temperature" [7, 8], it is hard to believe that the effective temperature could reach over 1000 °C. The fact that the transformation of gibsite (or boehmite) to corundum is not direct but undergoes a sequence of phases as in the heating experiments implies that the internal energy of the starting phase is raised by ball milling as a result of atom disordering (we observed an appreciable amount of line broadening) and of the rise in the local effective temperature. When the disordered phase attains a state of higher energy than the next phase in the transition sequence (3), a transformation takes place.

At present we are not able to explain why during the milling of boehmite the phases χ and κ appeared as transition phases and not γ and δ, as observed in heating-induced sequence (2).

During the milling and before the final conversion to α phase, the XRD patterns always showed the coexistence of two phases: boehmite (or gibbsite) and χ, or χ and κ, or κ and α. We believe that this behaviour resulted from the non-uniform milling and does not usually occur.

TEM and HREM examination confirmed the ball-milling-induced boehmite-to-corundum transition, and that the α-Al_2O_3 grain sizes are much smaller in milled than in heated powder.

5. Conclusion

The ball-milling-induced transition sequence from boehmite (or gibbsite) to α-Al_2O_3 was found to be

$$\left.\begin{array}{ll}\text{boehmite} & \text{AlOOH}\\ \hline \text{gibbsite} & \text{Al(OH)}_3\end{array}\right\} \rightarrow \chi\text{-Al}_2\text{O}_3 \rightarrow \kappa\text{-Al}_2\text{O}_3$$

$$\rightarrow \alpha\text{-Al}_2\text{O}_3$$

showing (a) similarity with the heating-induced sequences (1) and (2) and (b) that high energy ball milling could be equivalent to a thermal process.

References

1 A. Tonejc, C. Kosanović, A. M. Tonejc, M. Stubičar, B. Subotić, I. Smit and J. Bronić, *J. Alloys Compounds*, in press.

2 B. C. Lippens and J. H. de Boer, *Acta Crystallogr., 17* (1964) 1312.

3 S. C. Carniglia, *J. Am. Ceram. Soc., 66* (1983) 495.

4 S. J. Wilson and J. D. C. McConnell, *J. Solid State Chem., 34* (1980) 315.

5 Rong-Sheng Zhou and R. L. Snyder, *Acta Crystallogr., Sect. B, 47* (1991) 617.

6 V. Sarasvati, G. V. N. Rao, G. V. Rama Rao, *J. Mater. Sci., 22* (1987) 2529.

7 M. L. Trudeau, R. Schultz, D. Dussault and A. Van Neste, *Phys. Rev. Lett., 64* (1990) 93.

8 A. Tonejc, A. M. Tonejc and D. Duževič, *Scr. Metall. Mater., 25* (1991) 1111.

9 H. Yang and H. Bakker, *J. Alloys Compounds, 189* (1992) 113.